

Multiparametric MRI in differentiating pulmonary artery sarcoma and pulmonary thromboembolism: a preliminary experience

Min Liu
Chunhai Luo
Ying Wang
Xiaojuan Guo
Zhanhong Ma
Yuanhua Yang
Tianjing Zhang

PURPOSE

We aimed to define multiparametric magnetic resonance imaging (MRI) findings to differentiate between pulmonary artery sarcoma (PAS) and pulmonary thromboembolism (PTE).

METHODS

Eleven patients with suspected PTE were prospectively included to undergo pulmonary MRI before surgery or biopsy. MRI protocol included an unenhanced sequence, diffusion-weighted imaging (DWI, $b=800$ s/mm²) and a dynamic contrast-enhanced sequence. Morphologic characteristics including distribution, filling defect, and intensity were observed on T1-, T2-, and fat-suppressed T2-weighted imaging, DWI, and contrast-enhanced MRI. Apparent diffusion coefficient (ADC) values were calculated.

RESULTS

Six patients were pathologically diagnosed as PAS and the other five as chronic PTE. There were no significant differences in age, gender, presenting symptoms, D-dimer, and N-terminal pro-brain natriuretic peptide between the two groups ($P > 0.05$). Among MRI findings that were tested for their ability to diagnose PAS, area under the curve (AUC) was significantly higher than 0.5 for main pulmonary artery involvement (AUC, 0.83 ± 0.13 ; $P = 0.011$), hyperintensity on fat-suppressed T2-weighted imaging (AUC, 0.82 ± 0.14 ; $P = 0.025$), hyperintensity on DWI (AUC, 0.88 ± 0.12 ; $P = 0.002$), contrast enhancement (AUC, 0.92 ± 0.10 ; $P < 0.001$) and pleural effusion (AUC, 0.82 ± 0.14 ; $P = 0.025$). Moreover, grape-like appearance in distal pulmonary artery and cardiac invasion had 100% specificity for diagnosis of PAS. However, ADC value of PAS was not significantly different than that of chronic PTE ($U, 12.00$; $P = 0.584$).

CONCLUSION

Hyperintense filling defect in main pulmonary artery on fat-suppressed T2-weighted imaging and DWI and contrast enhancement may help to discriminate PAS from PTE.

Pulmonary artery sarcoma (PAS) is a rare primary malignancy of pulmonary artery with poor prognosis. The main manifestation of PAS is a filling defect in pulmonary artery on computer tomography pulmonary angiography (CTPA) or magnetic resonance imaging (MRI) mimicking pulmonary thromboembolism (PTE) (1). [¹⁸F]fluorodeoxyglucose positron emission tomography (¹⁸F-FDG PET) may be useful in differentiating PTE and PAS (1, 2), but other research indicates that PAS may not always show ¹⁸F-FDG uptake (3). Blackmon et al. (4) has suggested that in patients who do not respond to the initial thrombolysis or anticoagulation, further investigation with gadolinium-enhanced MRI should be undertaken. Currently, most imaging findings were evaluated with CT or PET, but the characteristics of PAS and the differentiation of PAS and PTE on multiparametric MRI remain unclear. Therefore, our purpose was to observe MRI findings of PAS and to determine the MRI findings that allow its differentiation with PTE.

Methods

Patient selection

This was a single-center prospective study and was approved by the ethics committee of our hospital. Written informed consent was obtained from each patient. From January 2013 to October 2014, 11 consecutive patients (male/female, 7/4; median age, 47 years; range, 30–69 years) with suspected PTE were included in this study. Because of the initial suspicion of PTE, all patients underwent CTPA and were treated with thrombolysis or an-

From the Departments of Radiology (M.L. ✉ dirradiology@163.com, X.G., Z.M.), Clinical Pathology (Y.W.), and the Respiratory Diseases Research Center (Y.Y.), Beijing Chaoyang Hospital of Capital Medical University, Beijing, China; Department of Radiology (C.L.), the second affiliated Hospital of Xi'an Medical College, Xi'an City, China; Siemens MR Northeastern Collaboration Application Department (T.Z.), Siemens MRI Center, Beijing, China.

Received 15 December 2015; revision requested 29 March 2016; last revision received 10 May 2016; accepted 13 May 2016.

Published online 6 December 2016.
DOI 10.5152/dir.2016.15584

ticoagulation in other hospitals. However, since there was no release of clot burden on CTPA, no relief of clinical symptoms, and lack of response to thrombolysis or anticoagulation, they were referred to our hospital for further diagnosis and treatment. Patients underwent pulmonary MRI 3–10 days before they were referred for surgery or biopsy. The pathologic diagnosis was made in eight patients by surgery and in the remaining three patients by pulmonary angiography with transvenous catheter suction biopsy. Sixteen patients who did not undergo pulmonary MRI or did not receive pathologic diagnosis were excluded from the study.

Imaging protocol

Pulmonary artery MRI was performed with a 3.0 T scanner (Tim Trio, Siemens Healthcare) using dedicated cardiac software with a body-flex receiver coil and vectocardiogram triggering. After scout imaging with transversal T2-weighted half-fourier acquisition single-shot turbo spin echo (HASTE) sequence, the unenhanced scan protocol consisted of the following sequences: the transversal, coronal and/or oblique T1-weighted imaging (TR/TE, 750/28 ms; flip angle, 180°; bandwidth, 305 Hz/Px, FOV, 340×340 mm; slice thickness, 5 mm; matrix, 256×256; acceleration factor, 2), T2-weighted imaging (TR/TE, 745/72 ms; flip angle, 180°; bandwidth, 235 Hz/Px; FOV, 340×340 mm; slice thickness, 5 mm; matrix, 256×256; acceleration factor, 2) and fat-suppressed T2-weighted imaging (TR/TE, 2200/100 ms; flip angle, 140°; bandwidth, 300 Hz/Px; FOV, 340×340 mm; slice thickness, 5 mm; matrix, 256×256; acceleration factor, 2). Then, the transversal diffusion weighted images (DWI) were obtained using navigated interleaved multishot echo planar imaging (EPI) sequence with fat suppression (b , 0 and 800 s/mm²; TR/TE, 4000/66 ms; flip angle, 90°; band-

width, 2012 Hz/Px; FOV, 350×350 mm; slice thickness, 5 mm; matrix, 128×128; acceleration factor, 2). Next, dynamic breath-hold 3D gadolinium-enhanced MRI sequences were acquired with transversal T1-weighted imaging volume interpolated breath-hold examination (VIBE) sequence with fat suppression (TR/TE, 3.48/1.28 ms; flip angle, 9°; bandwidth, 460 Hz/Px; FOV, 360×360 mm; slice thickness, 5 mm; matrix, 320×320; acceleration factor, 2) after gadopentetate dimeglumine (Magnevist, Schering) was applied at 0.2 mmol/kg bodyweight at a rate of 2 mL/s using a power injector (Mallinckrodt).

MRI analysis

MRI findings regarding embolus distribution, morphologic characteristics, DWI, pre- and postcontrast intensity were reviewed by two radiologists, who were blinded to other clinical and pathologic information. A third radiologist evaluated the findings when the two radiologists were not in consensus about their diagnosis. Intensity of the lesion on unenhanced MRI images (categorized as hyperintensity, mild hyperintensity, isointensity, mild hypointensity and hypointensity) was compared with the intensity of the chest wall. Apparent diffusion coefficient (ADC) values were measured for each clearly demarcated lesion on Syngo workstation (syngoMMWP, Siemens AG) by drawing a circular region of interest (ROI) into pulmonary arterial lesions. Enhancement was evaluated for each clearly demarcated lesion by drawing a circular ROI into pulmonary arterial lesions by Mean Curve, commercial software on Syngo workstation.

Statistical analysis

Quantitative data were expressed as mean±standard deviation (SD) and/or median value, unless otherwise specified. Comparison of quantitative clinical and MRI findings between PTE and PAS was performed by nonparametric two-independent-sample Mann-Whitney U test. Comparison of qualitative MRI findings between PTE and PAS was performed by Chi-square test or Fisher's exact test. Receiver operating characteristic (ROC) curves were used to evaluate MRI findings in differentiating pulmonary arterial benign and malignant filling defects. All analyses were performed with MedCalc Statistical Software version 14.8.1 (MedCalc Software). For all tests, $P < 0.05$ was considered statistically significant.

Results

Clinical characteristics of the patients are summarized in Table 1. After surgery, six cases (male/female, 5/1; median age 46 years; range, 36–69 years) were pathologically confirmed as PAS and the remaining five cases (male/female, 2/3; median age, 47 years; range, 40–50 years) as organized thrombus, which meant chronic PTE. Age ($U=13.0$, $P = 0.792$), gender ($P = 0.242$), and body mass index ($U=11.5$, $P = 0.485$) were not significantly different between chronic PTE and PAS patients. In our hospital, the median of D-dimer of chronic PTE patients was comparable to that of PAS patients ($U=10.0$, $P = 0.429$). There was no significant difference on N-terminal pro-brain natriuretic peptide (NT-proBNP) between the two groups ($U=11.0$, $P = 0.537$). The median duration from initial symptom to pathologic confirmation was nine months (range, 2–25 months).

Table 2 shows the distribution and morphologic characteristics of the lesions. The distribution of PAS and chronic PTE lesions were similar ($\chi^2=6.160$, $P = 0.188$), but the frequency of the main pulmonary artery involvement was significantly higher in the PAS group ($P = 0.045$). Six PAS lesions and three chronic PTE lesions manifested as columnar filling defects in the pulmonary artery (Figs. 1–3). The wall eclipsing sign (Figs. 1 and 3) was observed in five PAS and two chronic PTE lesions, with no significant difference between PAS and chronic PTE ($P = 0.242$). The proximal margins of three PAS (Fig. 2) and four chronic PTE (Fig. 3) lesions were smooth, while those of the remaining three PAS lesions (Fig. 1) and one chronic PTE lesion were irregular. Shape of the margin was not significantly different between PAS and chronic PTE ($P = 0.545$). In three PAS patients, MRI showed intraluminal filling defects in the main pulmonary trunk, left pulmonary artery or right pulmonary artery extending to the segmental and sub-segmental arteries with local aneurysmal dilatations, which we termed the sign of grape-like appearance (Fig. 2d). However, the sign of grape-like appearance was comparable in PAS and chronic PTE ($P = 0.240$). In addition, the frequency of pleural effusion in PAS was significantly more than chronic PTE ($P = 0.015$).

Intensity of PAS and chronic PTE lesions on MRI are shown in Table 3. On T1-weighted ($P = 0.424$) and T2-weighted images ($\chi^2=1.118$, $P = 0.561$) lesion intensity was comparable between chronic PTE and PAS.

Main points

- MRI findings of pulmonary artery sarcoma include hyperintense filling defect in the main pulmonary artery on fat suppressed T2-weighted and diffusion-weighted imaging and contrast enhancement.
- The grape-like appearance in distal pulmonary artery and cardiac invasion on MRI are the specific findings for pulmonary artery sarcoma.

Table 1. Clinical information of patients with suspected pulmonary thromboembolism

Patient	Gender	Age (years)	BMI (kg/m ²)	Symptom	Initial diagnosis	Initial treatment	D-dimer (mg/L)	NT-proBNP (pg/mL)	Duration* (months)	Surgery	Pathologic diagnosis
1	Male	50	24	Hemoptysis, chest pain, dyspnea	Acute PTE	Anticoagulation	0.42	153.2	8	PEA	Organized thrombus
2	Female	46	20	Chest pain, weight-loss	Acute PTE	Anticoagulation	0.37	241.7	3	PEA	Organized thrombus
3	Male	47	22	Chest pain, hemoptysis	Acute PTE	Thrombolysis	0.25	2128.2	25	PEA	Organized thrombus
4	Female	59	21	Dyspnea	Chronic PTE	Anticoagulation	0.14	2955	20	PEA	Organized thrombus
5	Female	40	22	Dyspnea, weight-loss	Chronic PTE	Anticoagulation	0.63	729.3	24	PEA	Organized thrombus
6	Female	69	22	Chest pain, dyspnea, hemoptysis	Acute PTE	Anticoagulation	0.51	2959	2	TCSB	Intimal sarcoma
7	Male	47	25	Chest pain	Acute PTE	Anticoagulation	2.39	161.2	10	TCSB	Intimal sarcoma
8	Male	45	22	Cough, dyspnea, fever	Acute PTE	Anticoagulation	0.23	58	10	PEC	Fibrosarcoma
9	Male	30	22	Chest pain, hemoptysis, fever	Acute PTE	Anticoagulation	0.55	137	9	PEC	Intimal sarcoma
10	Male	59	22	Cough, chest pain, dyspnea	Acute PTE	Anticoagulation	0.21	374.3	3	TCSB	Intimal sarcoma
11	Male	36	21	Cough, hemoptysis, chest pain, weight-loss	Acute PTE	Thrombolysis	9.47	2384	9	PEC	Fibrosarcoma

BMI, body mass index; NT-proBNP, N-terminal pro-brain natriuretic peptide; PTE, pulmonary thromboembolism; PEA, pulmonary endarterectomy; TCSB, transvenous catheter suction biopsy; PEC, pneumonectomy.

*duration was defined as the time between the initial symptoms and surgery.

Table 2. Morphologic and precontrast MRI findings of pulmonary artery sarcoma and pulmonary thromboembolism

Patient	Distribution	Morphologic characteristics	Proximal margin	Wall eclipsing sign	Distal PA	Cardiac invasion	Pericardial effusion	Pleural effusion
1	RPA	Columnar	Smooth	Yes	Stenosis	No	No	No
2	RPA	Columnar	Irregular	No	Stenosis	No	No	No
3	LPA	Columnar	Smooth	Yes	Stenosis	No	Yes	No
4	RPA	Eccentric	Smooth	No	Stenosis	No	No	No
5	RPA+LPA	Eccentric	Smooth	No	Stenosis	No	Yes	No
6	MPA+RPA	Columnar	Irregular	Yes	Stenosis	PV	Yes	Yes
7	MPA+RPA+LPA	Columnar	Irregular	Yes	Grape-like appearance	PV	No	No
8	RPA	Columnar	Smooth	Yes	Grape-like appearance	No	Yes	Yes
9	RPA	Columnar	Smooth	No	Stenosis	No	No	Yes
10	MPA+RPA	Columnar	Irregular	Yes	Stenosis	No	No	Yes
11	MPA+RPA+LPA	Columnar	Smooth	Yes	Grape-like appearance	No	Yes	Yes

PA, pulmonary artery; RPA, right pulmonary artery; LPA, left pulmonary artery; MPA, main pulmonary artery; PV, pulmonary valve.

On fat-suppressed T2-weighted imaging, three chronic PTE lesions were isointense, while five PAS lesions were hyperintense, and the remaining one was mildly hyperintense. On fat-suppressed T2-weighted imaging, intensity of the lesions were significantly different between chronic PTE and PAS

($\chi^2=6.722$, $P=0.041$). On DWI, lesion intensities of chronic PTE and PAS were significantly different ($\chi^2=7.693$, $P=0.022$); however, no significant difference was observed in ADC values between PAS (ADC value, 2.00×10^{-3} mm²/s) and chronic PTE groups (ADC value, 1.99×10^{-3} mm²/s) ($U=12.00$, $P=0.584$). On

contrast-enhanced MRI, chronic PTE did not demonstrate enhancement (Fig. 3), while five PAS lesions were significantly enhanced (Figs. 1 and 2) ($P=0.015$).

As shown in Table 4, among MRI findings that were tested for their ability to diagnose PAS, AUC was significantly higher than 0.5

Table 3. Intensity of pulmonary artery sarcoma and pulmonary thromboembolism on MRI

Patient	T1WI	T2WI	Fat-suppressed T2WI	DWI	ADC value (×10 ⁻³ mm ² /s)	Enhancement
1	Mildly high	Mildly high	Mildly high	Mildly low	1.63	No
2	Mildly high	Mildly high	Mildly high	Mildly high	1.42	No
3	Isointense	Isointense	Isointense	Mildly low	2.80	No
4	Isointense	Isointense	Isointense	Mildly low	2.62	No
5	Isointense	Isointense	Isointense	Mildly low	2.00	No
6	Isointense	Mildly high	High	Mildly high	3.72	Yes
7	Isointense	Isointense	High	Mildly high	3.78	Yes
8	Isointense	Mildly high	High	Mildly high	1.63	Yes
9	Isointense	high	High	Mildly high	2.03	Yes
10	Mildly high	Mildly high	Mildly high	Isointense	1.97	Yes
11	Isointense	Isointense	High	Mildly high	1.92	No

T1WI, T1-weighted imaging; T2WI, T2-weighted imaging; DWI, diffusion-weighted imaging; ADC, apparent diffusion coefficient.

Table 4. Receiver operating characteristic curves of MRI findings to predict pulmonary artery sarcoma

MRI findings	Sensitivity (%)	Specificity (%)	Youden index J	AUC	95% CI	P
MPA involvement	66.7	100	0.67	0.83±0.13	0.50–0.98	0.011*
Distribution	33.3	80	0.13	0.57±0.18	0.25–0.85	0.711
Dilated filling defect	66.7	80	0.47	0.67±0.17	0.33–0.91	0.337
Irregular proximal margin	50	80	0.30	0.65±0.17	0.32–0.90	0.385
Grape-like appearance of the distal PA	50	100	0.50	0.75±0.15	0.41–0.95	0.104
Wall eclipsing sign	83.3	60	0.43	0.72±0.17	0.38–0.94	0.193
Cardiac invasion	33.3	100	0.33	0.67±0.17	0.33–0.91	0.323
Pericardial effusion	50	60	0.10	0.55±0.18	0.24–0.84	0.783
Pleural effusion	83.3	80	0.63	0.82±0.14	0.48–0.97	0.025*
T1WI intensity	83.3	40	0.23	0.62±0.18	0.29–0.88	0.515
T2WI intensity	66.7	60	0.27	0.60±0.18	0.28–0.87	0.585
Fat-suppressed T2WI intensity	88.3	80	0.63	0.82±0.14	0.48–0.98	0.025*
DWI	100	80	0.80	0.88±0.12	0.56–0.99	0.002*
Enhancement	83.3	100	0.83	0.92±0.10	0.59–0.99	<0.001*

AUC, area under the receiver curve; 95% CI, 95% confidence interval; MPA, main pulmonary artery; PA, pulmonary artery; T1WI, T1-weighted imaging; T2WI, T2-weighted imaging.
*P < 0.05.

for the main pulmonary artery involvement, hyperintensity on fat-suppressed T2-weighted imaging and DWI, contrast enhancement, and pleural effusion. Moreover, other MRI findings including the sign of grape-like appearance and cardiac invasion were 100% specific to PAS.

Discussion

In this study, we observed multiparametric MRI findings of PAS and the differentiation of PAS and PTE. Hyperintense filling defect invading the main pulmonary arteries

on fat-suppressed T2-weighted imaging, contrast enhancement, and grape-like appearance in distal pulmonary arteries were the major findings of PAS on MRI.

Previous studies demonstrated that PAS typically affects middle-aged people, with a slight propensity for women (1, 5). In our study, PAS also mainly affected middle-aged people, but there was no significant difference in age between PTE and PAS patients. Moreover, most of our patients with PAS were men. Since PAS is quite difficult to distinguish from PTE based on clinical symptoms

and CT or magnetic resonance angiographic findings, we used multiparametric MRI. In order to reduce the influence of cardiac and respiratory motion on image quality, multiparametric MRI including vectocardiogram triggering and breath-hold on T2-weighted imaging, T2-weighted imaging, and fat-suppressed T2-weighted imaging were used instead of magnetic resonance angiography in this study. Moreover, Navigator echo technique used in DWI can effectively track rigid-body motion of limited amplitude and promise to obtain the same slice (6).

The filling defect occupying the main or proximal pulmonary arteries was reported to be a specific finding of PAS (7–9). In the current study, we found the filling defect in the main pulmonary artery to be a specific sign of PAS, which was not seen in any patients with PTE. PAS is reported as a disease of unilateral distribution whereas PTE is reported as a disease of bilateral distribution (10, 11). However, the distributions in PAS and PTE in our cases were not different. The grape-like appearance was a result of intraluminal filling defects in the main pulmonary artery trunk, left pulmonary artery or right pulmonary artery extending to the segmental and sub-segmental arteries, which had local aneurysmal dilatations. This sign was 100% specific to PAS; we believe this feature is related to the malignant nature of sarcoma, which grows rapidly and invades the segmental and sub-segmental pulmonary arteries. Although irregular margin was thought to be a feature of the malignant tumor, the proximal margin of both PAS and PTE could be smooth. Thus, it was not feasible to differentiate PAS from PTE using this feature. On CTPA, Gan et al. (12) suggested that the wall eclipsing sign is pathognomonic for PAS. They defined three manifestations of the wall eclipsing sign as: *i*) almost full occupation of the lumen of the pulmonary trunk, left pulmonary artery, or right pulmonary artery by a low density mass; *ii*) protrusion of the proximal end of this mass towards the right ventricular outflow tract; *iii*) eclipsing of one or both walls of the pulmonary trunk, left pulmonary artery, or right pulmonary artery by this lesion. On MRI, three PAS lesions and two PTE lesions demonstrated full occupation of the lumen of the pulmonary trunk, and the other two PAS lesions affected the pulmonary valves. Our ROC analysis suggests that the wall eclipsing sign on MRI is not a reliable sign for differentiating PAS and PTE. We believe this is because the spatial resolution of pulmonary arterial wall is better on MRI than on CT.

MRI has been used to differentiate benign from malignant portal vein thrombus (13) and cardiac tumor (14). In our cases, both

PAS and PTE lesions showed mild hyperintensity or isointensity on T1- and T2-weighted imaging. We do not think that T1- and

T2-weighted imaging are helpful to differentiate PAS from PTE. On fat-suppressed T2-weighted imaging, PAS lesions were hyperintense; however, PTE could display different signal intensities. According to our ROC analysis, hyperintensity on fat-suppressed T2-weighted imaging may be a helpful sign for identifying PAS. We speculate that the intensity of PTE on fat-suppressed T2-weighted imaging is related to various stages of thrombus (15). Characterization of tissue as benign or malignant by DWI is enabled by restricted water molecule diffusion in the malignant tissue, yielding lower ADC values than those of benign lesions (16). One study reported that ADC values of malignant portal vein thrombus (PVT) were significantly lower than bland PVT (13), while another study suggested that DWI was not reliable to differentiate benign PVT from malignant PVT (17). In the current study, most PAS lesions were hyperintense and PTE lesions were mildly hypointense on DWI. ROC analysis suggested that hyperintensity on DWI could be a sign of PAS. However, there was substantial overlap of ADC values between PAS and PTE. This result is in agreement with Sandrasegaran et al. (13) who found that ADC value of PVT is not a significant parameter to differentiate PVT from benign PVT. We

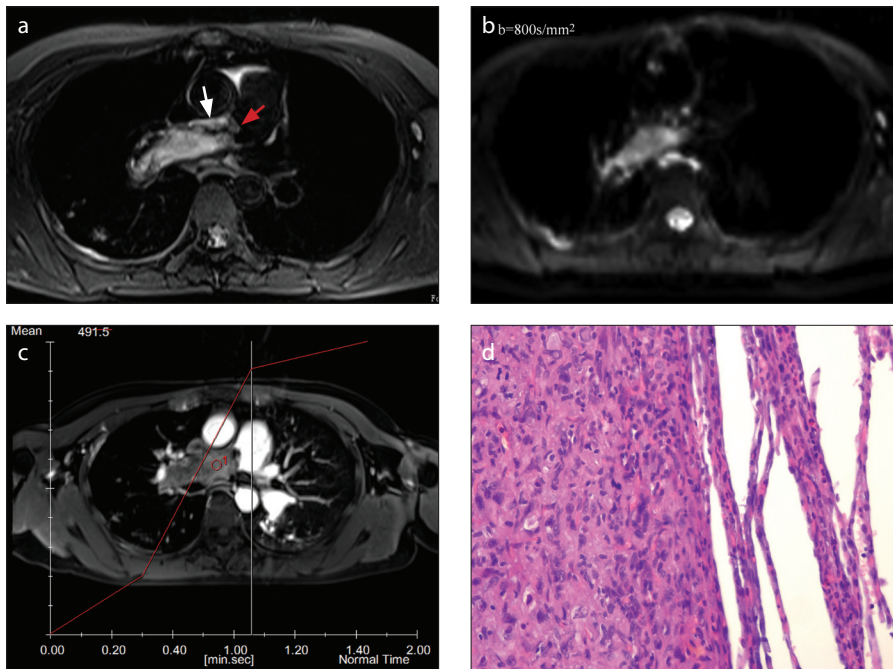


Figure 1. a–d. A 69-year-old woman with intimal sarcoma. On fat-suppressed T2-weighted imaging (a), the lesion is seen as a hyperintense columnar filling defect, with irregular proximal margin (red arrow) and the wall eclipsing sign (white arrow) in the main pulmonary artery and the right pulmonary artery. On DWI ($b=800 \text{ s/mm}^2$) (b), the lesion is hyperintense. On contrast-enhanced MRI (c), the lesion is heterogeneously enhanced. Histopathology (d) shows an abundance of malignant spindle cells with high cellularity and a high nuclear/cytoplasmic ratio (hematoxylin-eosin [HE] staining, $\times 400$).

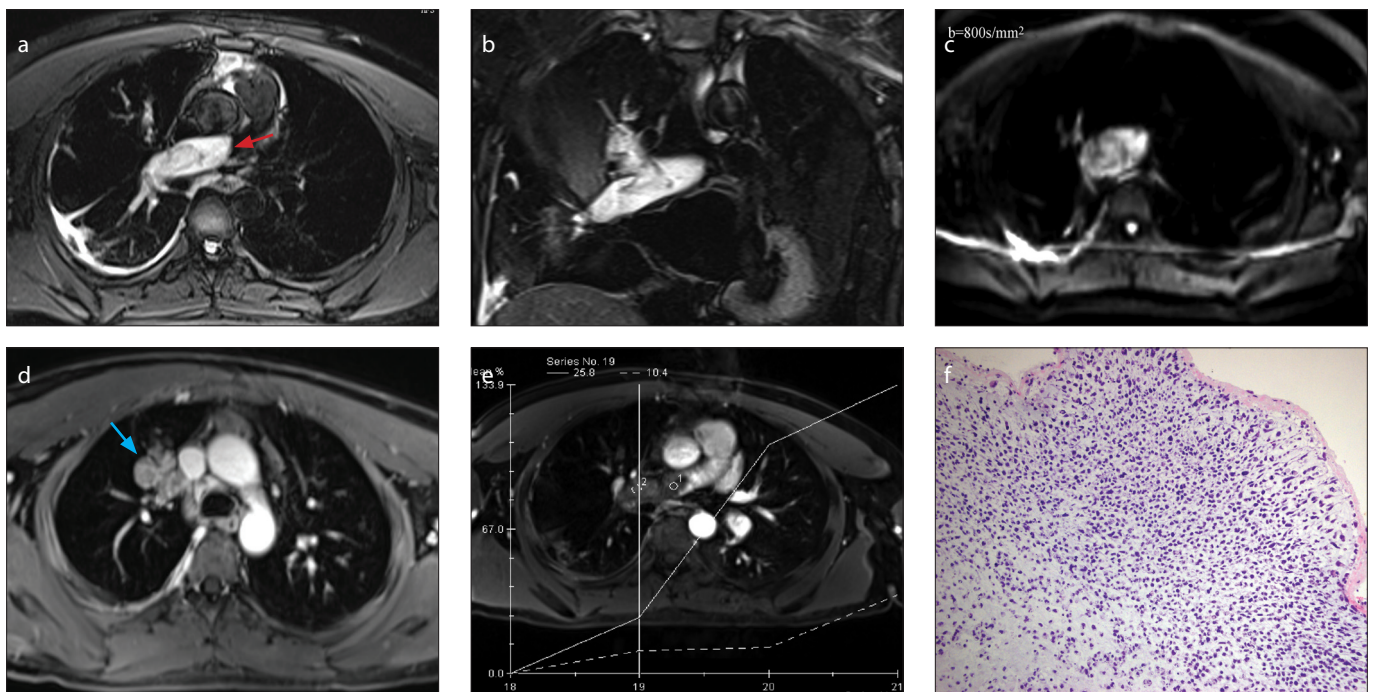


Figure 2. a–f. A 30-year-old man with intimal sarcoma. On transversal (a) and coronal (b) fat-suppressed T2-weighted imaging, the dilated filling defect in the right pulmonary artery is hyperintense and extends to the right upper lobe pulmonary artery (red arrow). DWI ($b=800 \text{ s/mm}^2$) (c) shows the lesion as mildly hyperintense. Contrast images (d, e) show that the lesion filled the right upper lobe pulmonary artery along its course giving it a grape-like appearance (blue arrow); the lesion is significantly enhanced (e). Histopathology (f) demonstrates an abundance of malignant spindle cells with high cellularity and a high nuclear/cytoplasmic ratio (HE staining, $\times 200$).

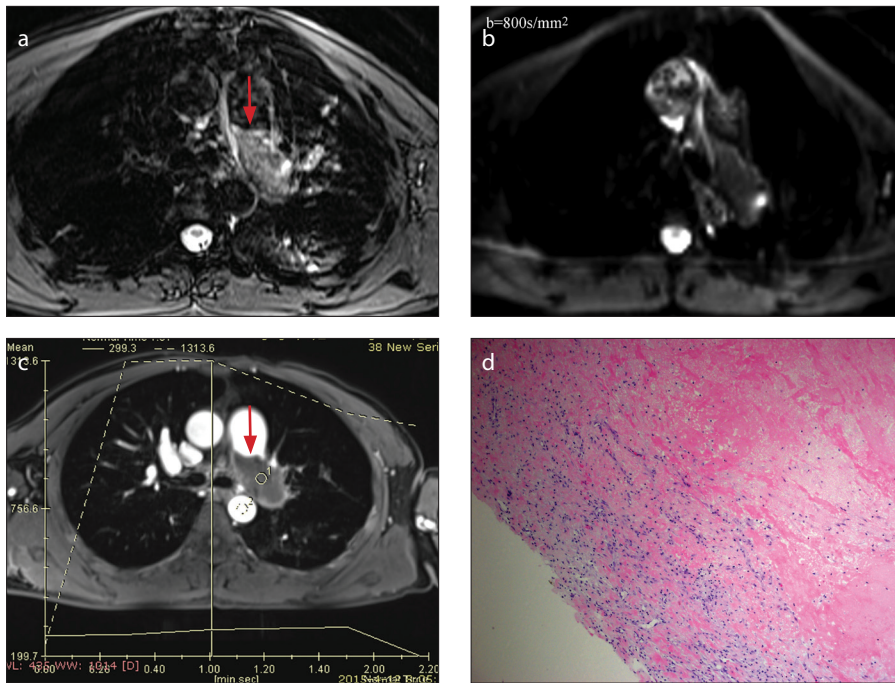


Figure 3. a–d. A 47-year-old man with organized thrombi, which appear as a columnar filling defect in left pulmonary artery. On fat-suppressed T2-weighted imaging (a), the lesion is isointense. On DWI ($b=800 \text{ s/mm}^2$) (b), the lesion appears hypointense. On contrast-enhanced image (c), proximal margin of the lesion is smooth (red arrow) and not enhanced. Histopathology (d) demonstrates abundant fibrin without malignant cells (HE staining, $\times 200$).

speculate that the lack of difference in the ADC values between PAS and PTE may be due to gradient-echo imaging, clot structure, T2 blackout effect, or the small sample size in this study. Some studies demonstrated that contrast enhancement of PVT on MRI was able to discriminate between malignant and bland PVTs (18, 19). However, another study suggested that both PAS and chronic PTE could be enhanced (20). In our study, contrast enhancement was observed in five of six PAS lesions, which is in agreement with the study by Cox et al. (8). However, one PAS lesion did not show obvious enhancement. Since sarcoma could coexist with thrombus, we think that enhancement of PAS depends on pathologic type and the components of tumor cells and thrombus tissue. In contrast-enhanced MRI, none of the PTE lesions were significantly enhanced, as compared with PAS. ROC analysis revealed that the enhancement on MRI could be a reliable finding of PAS. There were two types of sarcomas; however, we failed to compare their different MRI findings and correlate MRI and pathologic findings for such small number of cases included in this study.

Our study has several limitations. The first limitation is its small sample size; thus, some MRI findings were not statistically different

between PAS and PTE, such as cardiac invasion and the grape-like appearance in the involved distal pulmonary artery, although its specificity for PAS is 100%. Second, we only used a b value of 800 s/mm^2 ; therefore, how many b values are needed and which one should be better to discriminate PAS and PTE remain unknown. Third, only chronic PTE patients were compared with PAS; MRI findings of acute PTE and its differentiation with chronic PTE and PAS need further observation.

In conclusion, the most important MRI findings of PAS were hyperintense columnar filling defects occupying the lumen of the main or the proximal pulmonary artery on fat-suppressed T2-weighted imaging, contrast enhancement, and grape-like appearance in segmental pulmonary arteries. Although PAS lesions are easily misdiagnosed as PTE, the above MRI findings may be suggestive of PAS.

Acknowledgements

We thank members of all participating departments. We thank Professor Lirong Liang for advice on data management and for valuable suggestions about statistical analysis. This research is supported by Chinese National Scientific Research Foundation (30900364), Beijing Young Resident Researching Foundation (2014-3-026), Chinese National 12th Five-Year Researching Plan (2011BA11B17) and National Public Science and Technology Funds Projects

(201402019). Funders had no role in study design, data collection and analysis, decision to publish, or preparation of the manuscript.

Conflict of interest disclosure

The authors declared no conflicts of interest.

References

1. Bendel EC, Maleszewski JJ, Araoz PA. Imaging sarcomas of the great vessels and heart. *Semin Ultrasound CT MR* 2011; 32:377–404. [CrossRef]
2. Tueller C, Fischer Biner R, Minder S, et al. FDG-PET in diagnostic work-up of pulmonary artery sarcomas. *Eur Respir J* 2010; 35:444–446. [CrossRef]
3. Benz MR, Tchekmedyan N, Eilber FC, et al. Utilization of positron emission tomography in the management of patients with sarcoma. *Curr Opin Oncol* 2009; 21:345–351. [CrossRef]
4. Blackmon SH, Rice DC, Correa AM, et al. Management of primary pulmonary artery sarcomas. *Ann Thorac Surg* 2009; 87:977–984. [CrossRef]
5. Krüger I, Borowski A, Horst M, et al. Symptoms, diagnosis, and therapy of primary sarcoma of the pulmonary artery. *Thorac Cardiovasc Surg* 1990; 38:91–95. [CrossRef]
6. Wang Y, Rossmann PJ, Grimm RC, Riederer SJ, Ehman RL. Navigator-echo-based real time and triggering for reduction of respiration effects in three dimensional coronary MR angiography. *Radiology* 1996; 198:55–60. [CrossRef]
7. Yi CA, Lee KS, Choe YH, Han D, Kwon OJ, Kim S. Computed tomography in pulmonary artery sarcoma distinguishing features from pulmonary embolic disease. *J Comput Assist Tomogr* 2004; 28:34–39. [CrossRef]
8. Cox JE, Chiles C, Aquino SL, Savage P, Oaks T. Pulmonary artery sarcomas: A review of clinical and radiologic features. *J Comput Assist Tomogr* 1997; 21:750–755. [CrossRef]
9. Smith WS, Lesar MS, Travis WD, Lubbers P, et al. MR and CT findings in pulmonary artery sarcoma. *J Comput Assist Tomogr* 1989; 13:906–909. [CrossRef]
10. Wittram C, Maher MM, Yoo AJ, Kalra MK, Shepard JA, McCloud TC. CT angiography of pulmonary embolism: diagnostic criteria and causes of misdiagnosis. *Radiographics* 2004; 24:1219–1238. [CrossRef]
11. Chow B, Wittram C, Lee VW. Unilateral absence of pulmonary perfusion mimicking pulmonary embolism. *AJR Am J Roentgenol* 2001; 176:712. [CrossRef]
12. Gan HL, Zhang JQ, Huang XY, Yu W. The wall eclipsing sign on pulmonary artery computed tomography angiography is pathognomonic for pulmonary artery sarcoma. *PLoS One* 2013; 8:e83200. [CrossRef]
13. Sandrasegaran K, Tahir B, Nutakki K, et al. Usefulness of conventional MRI sequences and diffusion-weighted imaging in differentiating malignant from benign portal vein thrombus in cirrhotic patients. *AJR Am J Roentgenol* 2013; 201:1211–1219. [CrossRef]
14. Bogaert J, Dymarkowski S. Cardiac Masses. In: Bogaert J, Dymarkowski S, Taylor AM, Muthurangu V, eds. *Clinical cardiac MRI*. 2nd ed. Berlin:Springer-Verlag, 2012; 411–464. [CrossRef]

15. Vidmar J, Kralj E, Bajd F, Serša I. Multiparametric MRI in characterizing venous thrombi and pulmonary thromboemboli acquired from patients with pulmonary embolism. *J Magn Reson Imaging* 2015; 42:354–361. [\[CrossRef\]](#)
16. Koh DM, Collins DJ. Diffusion-weighted MRI in the body: applications and challenges in oncology. *AJR Am J Roentgenol* 2007; 188:1622–1635. [\[CrossRef\]](#)
17. Catalano OA, Choy G, Zhu A, Hahn PF, Sahani DV. Differentiation of malignant thrombus from bland thrombus of the portal vein in patients with hepatocellular carcinoma: application of diffusion-weighted MR imaging. *Radiology* 2010; 254:154–162. [\[CrossRef\]](#)
18. Tublin ME, Dodd GD 3rd, Baron RL. Benign and malignant portal vein thrombosis: differentiation by CT characteristics. *AJR Am J Roentgenol* 1997; 168:719–723. [\[CrossRef\]](#)
19. Okumura A, Watanabe Y, Dohke M, et al. Contrast-enhanced three-dimensional MR portography. *Radiographics* 1999; 19:973–987. [\[CrossRef\]](#)
20. Wittram C, Maher MM, Halpern E, et al. The Hounsfield unit values of acute and chronic pulmonary emboli (abstr). In: Radiological Society of North America scientific assembly and annual meeting program. Oak Brook, Ill: Radiological Society of North America, 2003; 678.